

Pyruvate Dehydrogenase Kinase Isoform 2 Activity Limited and Further Inhibited by Slowing Down the Rate of Dissociation of ADP[†]

Haiying Bao, Shane A. Kasten, Xiaohua Yan,[‡] and Thomas E. Roche*

Department of Biochemistry, Kansas State University, Manhattan, Kansas 66506

Received March 15, 2004; Revised Manuscript Received August 18, 2004

ABSTRACT: Pyruvate dehydrogenase kinase 2 (PDK2) activity is enhanced by the dihydrolipoyl acetyltransferase core (E2 60mer) that binds PDK2 and a large number of its pyruvate dehydrogenase (E1) substrate. With E2-activated PDK2, K⁺ at ~90 mM and Cl⁻ at ~60 mM decreased the K_m of PDK2 for ATP and competitive K_i for ADP by ~3-fold and enhanced pyruvate inhibition. Comparing PDK2 catalysis \pm E2, E2 increased the K_m of PDK2 for ATP by nearly 8-fold (from 5 to 39 μ M), increased k_{cat} by ~4-fold, and decreased the requirement for E1 by at least 400-fold. ATP binding, measured by a cold-trapping technique, occurred at two active sites with a K_d of 5 μ M, which equals the K_m and K_d of PDK2 for ATP measured in the absence of E2. During E2-aided catalysis, PDK2 had ~3 times more ADP than ATP bound at its active site, and the pyruvate analogue, dichloroacetate, led to 16-fold more ADP than ATP being bound (no added ADP). Pyruvate functioned as an uncompetitive inhibitor versus ATP, and inclusion of ADP transformed pyruvate inhibition to noncompetitive. At high pyruvate levels, pyruvate was a partial inhibitor but also induced substrate inhibition at high ATP levels. Our results indicate that, at physiological salt levels, ADP dissociation is a limiting step in E2-activated PDK2 catalysis, that PDK2·[ADP or ATP]·pyruvate complexes form, and that PDK2·ATP·pyruvate·E1 reacts with PDK2·ADP·pyruvate accumulating.

The mitochondrial pyruvate dehydrogenase complex (PDC)¹ catalyzes the irreversible conversion of pyruvate to acetyl-CoA and CO₂ and also generates NADH. The components that are required for the overall reaction include the pyruvate dehydrogenase (E1) component, the dihydrolipoyl acetyltransferase (E2), the dihydrolipoyl dehydrogenase (E3) component, and the E3-binding protein (E3BP) (1, 2). The fractional PDC activity is set by the competing activities of two classes of dedicated enzymes, the pyruvate dehydrogenase kinase (PDK) and pyruvate dehydrogenase phosphatase (PDP) (1, 2). Phosphorylation of the E1 component by PDK results in inactivation, and dephosphorylation by PDP results in reactivation. Inactivation limits and activation enhances the extent to which glucose-connected fuels undergo complete oxidation or are transformed to fatty acids (2–5).

PDK isozymes, together with the related branched-chain dehydrogenase kinase, comprise a novel family of serine kinases, unrelated to cytoplasmic Ser/Thr/Tyr kinases (2, 6–12). Four pyruvate dehydrogenase kinase (PDK) isozymes

(6–8) and two pyruvate dehydrogenase phosphatase (PDP) isoforms carry out these reactions (13, 14). Remarkably different effector sensitivities have been uncovered for the different PDK isoforms (2, 15–18). The functioning of each PDK isoform in salient roles is substantiated by the strong conservation of the primary structure of each isoform in mammals (2, 8, 9).

PDK2 is the most widely distributed among the four PDK isoforms (6, 15, 19) and is highly sensitive to the full set of known regulatory effectors of mammalian PDK activities (2, 15–18). PDK2 activity is markedly stimulated by NADH and acetyl-CoA and is inhibited by pyruvate and ADP. Stimulation contributes to feedback suppression of the PDC reaction when fatty acids and ketone bodies are being preferentially used as energy sources (2–5). This is critically important for conservation of carbohydrate reserves. As signals indicating abundant substrate and a low-energy state, pyruvate and ADP inhibit PDK2 activity. Hormone-induced or workload-fostered increases in glucose transport or glycogen breakdown coupled to glycolysis elevate pyruvate; increased cellular workload elevates ADP and P_i. Kinase activity is reduced by ADP and pyruvate and synergistically by the combination (20). Inorganic phosphate anion also fosters ADP and pyruvate inhibition (20). Pyruvate binds directly to PDKs (21) and can be replaced by the pyruvate analogue, dichloroacetate (20, 22). The latter has the advantage that it is not a substrate in the E1 reaction. Here, we further characterize the regulation of the PDK2 isoform by ADP and pyruvate.

The E2 component markedly increases the efficiency of PDK2 catalysis and intervenes to produce or modify all of

[†] This work was supported by National Institutes of Health Grant DK18320 and by the Agricultural Experiment Station, Contribution 04-280-J.

* To whom correspondence should be addressed. Phone: 785-532-6116. Fax: 785-532-7278. E-mail: bchter@ksu.edu.

[‡] Present address: Biochemistry and Molecular Biology, School of Public Health, The Johns Hopkins University, 622 N. Washington St., Baltimore, MD 21205.

¹ Abbreviations: PDC, pyruvate dehydrogenase complex; E1, pyruvate dehydrogenase component; E2, dihydrolipoyl acetyltransferase component; L1 domain, NH₂-lipoyl domain of E2; L2 domain, interior lipoyl domain of E2; E3, dihydrolipoyl dehydrogenase; E3BP, E3-binding protein; PDK, pyruvate dehydrogenase kinase; PDP, pyruvate dehydrogenase phosphatase; pyr, pyruvate.

these regulatory responses (16). E2 and E3BP assemble into a dodecahedron by association of their C-terminal domains. Our recent studies indicate this involves forming an E2₄₈·E3BP₁₂ oligomer (23). Outside this inner core, mobile linker regions connect first to an E1-binding domain in E2 and an E3-binding domain in E3BP; in each case, this is followed by mobile connections to two lipoyl domains in E2 and a single lipoyl domain in E3BP. The N-terminal lipoyl domain of E2 is designated L1, and the second lipoyl domain, L2. NADH and acetyl-CoA stimulate kinase activity by increasing the state of reduction and acetylation of the lipoyl domains, particularly the L2 domain (2, 16, 18, 24–27). E2 activation of PDK2 transforms PDK2 activity from being poorly inhibited by pyruvate or dichloroacetate to being markedly inhibited (16).

In solution PDK2 is a stable dimer and binds with a much stronger affinity to the L2 domains of E2 than the L1 domain or the lipoyl domain of the E3BP component (28). Stronger binding by the dimeric GST–L2 than monomeric L2 and the equivalence of the affinity of GST–L2 and E2 for PDK2 established that binding of PDK2 is strengthened by interaction of the dimeric PDK2 with two lipoyl domains (28). This bifunctional binding is further enhanced by reduction of L2's lipoyl group and to a small extent by E1 being bound to E2 (28). ADP or ATP decreases the affinity for PDK2 binding to E2 and the ATP analogue, AMP-PNP, and phosphorylation of E1 decreases binding of PDK2 to E2–E1 (28). We show that AMP-PNP is a very effective inhibitor of PDK2.

Beyond the critical roles of E2 in facilitating kinase function, previous studies on bovine kinases indicated that potassium, phosphate, and possibly Cl[−] at elevated but physiological levels significantly altered the capacities of effectors to influence PDK activity (16, 20, 24, 29, 30). In studies with a mixture of bovine PDKs, ADP inhibition was enhanced by elevated potassium ion (29), pyruvate inhibition was increased both by this condition and by phosphate anion (20), and stimulation by NADH and acetyl-CoA increased due to elevating KCl or potassium phosphate (24). With tight control of ions and ionic strength, this paper emphasizes the basic kinetic and binding properties of human PDK2 centered on ATP and ADP and the effects of pyruvate (or the pyruvate analogue, dichloroacetate). Kinetic studies are conducted in the presence and absence of E2. A mechanism for PDK2 regulation is supported in which kinase activity is limited by ADP dissociation and pyruvate binding, and reaction pathways lead to PDK2·ADP·pyruvate complex forming to further slow ADP dissociation. The companion paper (39) presents evidence that stimulation by NADH and acetyl-CoA speed up this step.

EXPERIMENTAL PROCEDURES

Materials. Recombinant human PDK2 (16), E2, E2·E3BP (28), and E3 (31) were prepared as described previously. Constructs of expression systems for human E1 with a removable His tag, E2, and E2·E3BP will be described elsewhere.² E1 was prepared free of TPP as previously described (16). This involved a combination of exhaustive washing of the E1 anchored by its His-tag to the Ni affinity

column and further dialysis treatment with 2 mM EDTA following elution of E1 and the removal of the His tag by treatment with PreScission protease. [γ -³²P]ATP and [α -³²P]ATP were purchased from New England Nuclear.

Kinase Activity Assays. PDK activity was measured in duplicate or triplicate as the initial rate of incorporation of [³²P]phosphate into E1 using 0.1 mM [γ -³²P]ATP (150–500 cpm/pmol) at 30 °C (16, 25, 26). Most assays used 0.04–0.1 μ g of PDK2 and measured incorporation after a 60 s reaction times (below). Assays that paralleled binding studies used more PDK2, lower reaction temperatures, and a shorter reaction time. Most assays were conducted with a “high salt” buffer A which had a final pH of 7.4 and the following composition and ionic strength (μ): 113 mM Hepes–Tris, pH 7.4 (μ = 50 mM), 60 mM KCl (μ = 60 mM), 30 mM K–Hepes (μ = 30 mM), 2 mM MgCl₂ (μ = 6 mM), 0.2 mM EDTA (μ = 0.5 mM), and finally 13.5 ± 2.7 mM K⁺ and 7.7 ± 1.5 mM phosphate (μ = 19.5 ± 3.8 mM); these final somewhat variable levels result from additions of E2 (in 50 mM potassium phosphate, pH 7.2) and E1 (in 50 mM potassium phosphate, pH 7.5). The total μ = 166 ± 4 mM and total K⁺ is 103.5 ± 3 mM, and unless otherwise indicated, assays mixtures in these studies also contained 2 mM dithiothreitol. Concentrated protein components were preincubated together for 60 min at 4 °C in the buffers in which they were prepared and then were added to reaction mixtures for 2 min at 30 °C prior to initiation of PDK2 activity. Unless otherwise indicated, exposure to the final specific salt conditions and to 2 mM dithiothreitol occurred only during the 2 min incubation at 30 °C prior to initiation of activity; however, E1 was prepared in the presence of 1 mM dithiothreitol, and E1 generally contributed about 40% of the volume of the preincubation mixtures. We evaluated the effects of K⁺ and Cl[−] counterions using two other buffers. K⁺ was decreased from ~103.5 to ~13.5 mM and 60 mM Cl[−] deleted in buffer B, which was made with a final concentration of 316 mM Hepes–Tris (μ = 140 mM) and had the same potassium phosphate, MgCl₂, and EDTA to give the same total μ of 166 ± 4 mM. Buffer A' lacked Cl[−] (beyond that provided with 2 mM MgCl₂) but had the same level of K⁺ as buffer A; buffer A' was made by substituting 60 mM K–Hepes for 60 mM KCl. All studies beyond those described in Table 1 and all binding studies (below) were conducted in buffer A. Other conditions were as indicated in figure and table legends. Incorporation of [³²P]phosphate was measured as previously described (25, 26). Assays were conducted at least in duplicate; average values are shown. In the great majority of assays, deviations from the average were less than ±4%.

For the data with E2 included, the results are fit either with a linear least squares or by the Sigma Plot 8.02 enzyme kinetics model. For the data without E2 in which ATP and E1 are varied, the kinetic data are fit by a modification of the Sigma Plot 8.02 program with enzyme kinetics module 1.1. We changed the ordered equilibrium bisubstrate equation to that for the ordered steady-state bisubstrate equation (added the equilibrium dissociation constant for the first substrate) and enabled the plotting of data with such modifications. The data were fit with different regression analyses. We show fits that were either linear least squares or weighted least squares (termed reciprocal v in this program). With the same preparations, kinetic constants

² Y. Hiromasa, H. Bao, X. Yan, X. Gong, A. Yakhnin, J. Dong, S. A. Kasten, L. Hu, T. Peng, J. C. Baker, M. Sadler, and T. E. Roche, manuscript in preparation.

Table 1: Changes in Kinetic Parameters of PDK2 in Phosphorylating E2-Bound E1 with Different Buffer Conditions and Preparations of PDK2 and E2^a

buffer (effector)	V_{max} ($\text{nmol}\cdot\text{min}^{-1}\cdot\text{mg}^{-1}$)	$K_m(\text{ATP})$ (μM)	K_i (μM)	k_{cat} (s^{-1})	k_{cat}/K_m ($\text{s}^{-1}\text{M}^{-1}$)
expt 1 (Figure 1A)					
A	1600 ± 50	103 ± 10		2.44	2.4×10^4
B	3100 ± 180	220 ± 30		4.7	2.1×10^4
expt 2 (Figure 1B)			ADP		
A (ADP)	1420 ± 200	105 ± 30	140 ± 20	2.2	2.1×10^4
B (ADP)	2305 ± 150	190 ± 15	520 ± 30	3.5	1.8×10^4
expt 3			ADP		
A	595 ± 40	39.5 ± 3	37 ± 3	0.91	2.3×10^4
A' (no Cl ⁻)	1190 ± 45	71 ± 3	62 ± 3	1.8	2.6×10^4
B	1400 ± 150	100 ± 8	125 ± 16	2.1	2.1×10^4
expt 4 ^b					
A	595 ± 25	38.5 ± 2.5		0.91	2.4×10^4
expt 5 (Figure 2)			AMP-PNP		
A	420 ± 35	25 ± 5	3.1 ± 0.7	0.65	2.6×10^4
expt 6 (Figure 5)			pyr ~95		
A	1005 ± 40	56.4 ± 1.5		1.5	2.7×10^4

^a The buffers and assay conditions were as described under Experimental Procedures and the indicated figure legends. In all cases, the protein components were preincubated together at 4 °C for >1 h and then exposed to 2 mM dithiothreitol for 2 min at 30 °C prior to initiation of PDK2 activity. ^b Control curve in Figure 2 of the companion paper (39).

derived from different experiments with the same buffer conditions (but often with variation in ligand levels) agree within experimental error. Experiments conducted with different preparations support the general conclusions; quantitative differences with different E2 preparations are described.

Binding of Adenine Nucleotides in the Absence and Presence of the Kinase Reaction. Using [α -³²P]ATP, binding of ATP to PDK2 was measured by a cold trapping technique (20). The technique has been significantly modified and used to estimate binding both in the absence and in the presence of catalytic turnover. When just binding was measured, 18 μg of E2 and 2 μg of PDK2 were incubated in buffer A at 22 °C for 90 s, and the indicated concentration of [α -³²P]ATP was added to give a final volume of 50 μL . Ligands, such as ADP and DCA, were added as described in the kinase assays above. For turnover assays, the level of E2 was increased to 39 μg , and 39 μg of E1 was added; the PDK2 level was maintained at 2 μg . In experiments involving turnover, parallel assays were performed with [α -³²P]ATP or [γ -³²P]ATP being added to the indicated final concentrations in 50 μL and allowed to react for 12–25 s at 22 °C. With or without turnover, a 45 μL sample was then diluted into 0.9 mL of 20 mM potassium phosphate buffer, pH 7.0, containing 5% glycerol that was maintained at -3 °C. The entire 945 μL was then applied to a Millipore filter (GS, 0.2 μm) just as a portion of the same -3 °C buffer nearly finished passing through the filter. This was followed immediately by washing with 9 mL of the -3 °C buffer. For binding without turnover, the membrane was removed and the bound radioactivity measured. For assays involving catalytic turnover, the kinase-bound adenine nucleotide was released from the filter by applying 2.5 mL of 5% formic acid. The ³²P in this fraction was then measured (Cerenkov counting). Binding was proportional to PDK2 (see inset to Figure 6); PDK2 was not released from the filter during the 9 mL wash. In the absence of turnover (no E1), the same level of binding was estimated by counting the membrane (not treated with formic acid) or by measuring the radioactivity released into the formic acid. Therefore, formic acid treatment fully releases the specifically bound adenine

nucleotide, which was also supported by counting the membrane after this treatment. In the absence of turnover, both ATP sources gave exactly the same results. With turnover, there was no contamination by phosphorylated E1 in the adenine nucleotide released by formic treatment. A portion of phosphorylated E1 was released during the wash with 9 mL of cold phosphate buffer; however, no residual phosphorylated E1 was released during the formic acid wash. Corrections from the minus PDK2 background assays were small. Under turnover conditions, the use of [α -³²P]ATP allowed the level of bound ATP plus ADP to be measured whereas the use of [γ -³²P]ATP only allows the level of bound ATP to be measured. All assays were conducted in duplicate; deviation ranges are shown by error bars. Repetitive or closely related experiments gave results that were within experimental error.

RESULTS AND DISCUSSION

Changes in V_{max} and the K_m for ATP with Elevation of Specific Ions at Constant Ionic Strength and Product Stimulation. Substantial variation in kinetic parameters of PDKs is caused by specific ion effects. This includes major effects on the kinetic parameters for substrate (ATP), inhibitors (ADP, pyruvate), and product stimulation by NADH and acetyl-CoA. At a nearly constant ionic strength ($\mu = 166 \pm 3$ mM), the effects of K⁺ and K⁺ + Cl⁻ on human PDK2 activity were evaluated using Tris and Hepes as counterions or in combination to create the target ionic strength. With E2-bound E1 as a substrate, the following assays were conducted with saturating E1³ so that true V_{max} and K_m values for ATP are obtained. However, we have observed considerable variation in these parameters; insights into the cause of that variation will be indicated below and resolved in the companion paper (39).

Figure 1 shows studies in which a particularly high V_{max} along with an elevated K_m for ATP is observed for PDK2, but more commonly our preparations of components have given lower values (Table 1). More important than the PDK2 preparation is the status of the E2, specifically the reduction state of the lipoyl groups and the time E2 retains even a

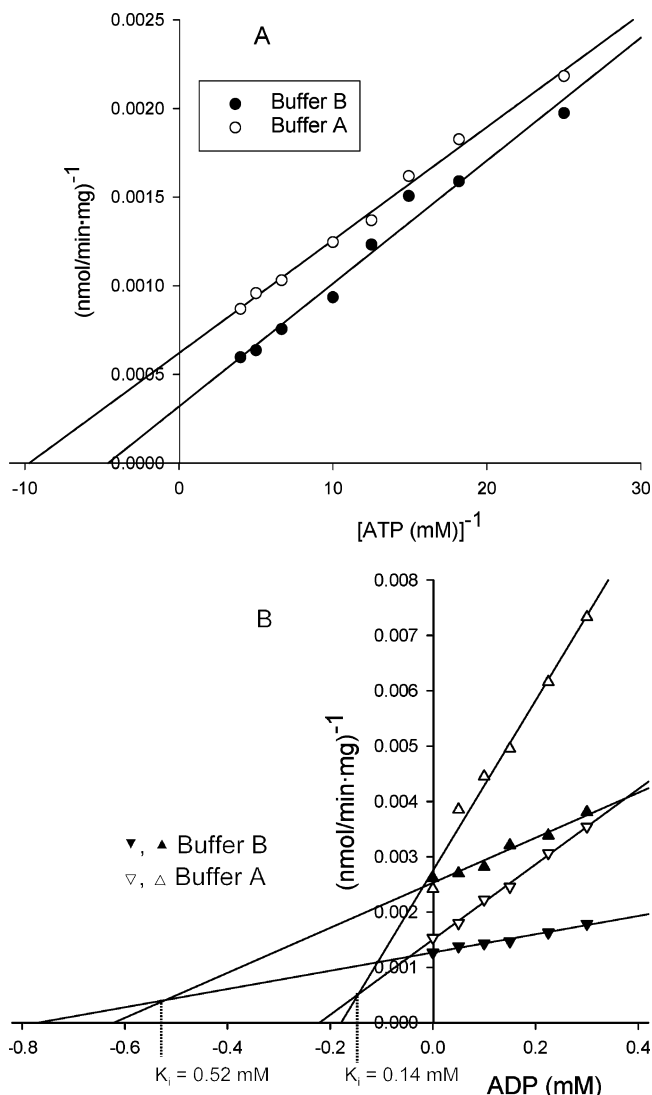


FIGURE 1: Double reciprocal plot of the variation in initial velocities of PDK2 with ATP level conducted in buffer A and buffer B (panel A) and Dixon plot of the change in PDK2 rates with the ADP concentration. For the study in panel A, E1, E2, and PDK2 were included at 10.5, 10, and 0.04 μg in 25 μL assays which were performed in duplicate at the indicated concentrations of $[\gamma\text{-}^{32}\text{P}]\text{ATP}$ in buffer A and buffer B. For the experiment in panel B, the same level of components were included, and sets of assays were conducted with 0.040 and 0.100 mM $[\gamma\text{-}^{32}\text{P}]\text{ATP}$ at the indicated concentrations of ADP. The K_i for ADP = $-x$ intersect at the crossover point for each pair of lines. Other conditions were as described under Experimental Procedures.

small portion of lipoyl groups in the reduced form [some observations below but demonstrated primarily in the companion paper (39)]. Figure 1A shows double reciprocal

³ Most of the assays use 10–14 μg of E1 with 10 μg of E2 in 25 μL . This corresponds to 0.112 μM E2 with 23.3–32.7 E1 per E2·E3BP. Two sets of data indicate that this provides a saturating level of E1. Dilution of complexes using 0.5 PDK2 dimer per E2·E3BP from 0.112 to 0.02 μM caused no change in the specific activity measured for PDK2 with 0.1 mM ATP and 23.3 E1 bound per E2·E3BP. PDK2 activity was quenched by hexokinase/glucose in <1 s and kinase-catalyzed inactivation of PDC measured with excess E2·E3BP and E3 (Y. Hiromasa and T. E. Roche, unpublished results). Also, with standard levels of E2 and 0.4 PDK dimer per E2 60mer, reducing the complement of bound E1 from 24 to 10 per E2 60mer does not cause a significant decrease in the initial rate of phosphorylation (^{32}P incorporation/12 s) by PDK2 or PDK3 (X. Yan and T. E. Roche, unpublished results).

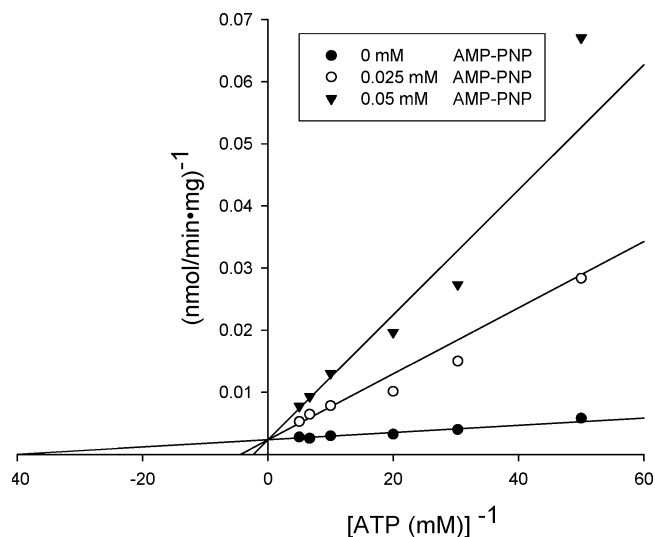


FIGURE 2: Analysis of inhibition by AMP-PNP by a double reciprocal plot of the variation in PDK2 activity with ATP concentration. Assays were conducted in buffer A with 0.07 μg of PDK2 with 0, 0.025, and 0.050 mM AMP-PNP; other conditions were as described in Figure 1. The data were fit using the Sigma Plot 8.02 enzyme kinetics module, treating AMP-PNP as a linear competitive inhibitor. Fitting this data set with noncompetitive inhibition (37) (mixed inhibition) with the intercept slightly to the side of the y axis gave similar residuals, but competitive inhibition was favored by our cumulative studies.

plots for two studies that gave very high V_{max} values for assays conducted using the low K^+ (13.5 mM), no Cl^- buffer B or buffer A containing both 103 mM higher K^+ and 60 mM Cl^- ions. Figure 1B shows a Dixon plot for ADP inhibition in these two buffers. Table 1 summarizes the results from studies conducted in the high-salt buffer A and the low-salt buffer B and in experiment 3 with buffer A', which lacks Cl^- but also had $\mu = 166 \text{ mM}$. For studies in buffer A, the results in experiment 3, Table 1, as well as the control curves with only ATP varied in Figure 2 (experiment 5, Table 1) and Figure 2 of the companion paper (experiment 4, Table 1), show more typical examples of lower V_{max} and ATP K_m values determined for PDK2. The lower salt buffer B invariably gave higher V_{max} and K_m values with the same component preparations (experiments 1–3, Table 1). With variation in parameters in buffer A, the k_{cat}/K_m ratio remained relatively constant at $\sim 2.5 \times 10^4 \text{ s}^{-1} \text{ M}^{-1}$. This suggests that the affinity of binding adenine nucleotide at the active site has a marked influence on the rate of the reaction with tighter binding reducing the reaction rate. When PDK2 gave V_{max} and K_m values in the typical range in buffer A (experiments 3–5, Table 1), use of the buffer lacking Cl^- at the same ionic strength gave higher V_{max} and K_m but below those in buffer B (experiment 3, Table 1). Cl^- seems to be an essential buffer component for observing significant stimulation by NADH and acetyl-CoA [see companion paper (39)].

Under all conditions ADP was a competitive inhibitor versus ATP. The results establish that the K_m for ATP and K_i for ADP of PDK2 decrease with a change in buffers from one with 13.5 mM potassium (buffer B) to one containing 114 mM K^+ plus 60 mM Cl^- (buffer A). With the high $V_{\text{max}}-K_m$ PDK2, there was a somewhat larger decrease in K_i (3.7-fold) than K_m (1.8-fold) for the transition to buffer A as compared to the low K^+ , no Cl^- buffer B (experiment

2, Table 1), whereas these parameters were closer (2.5- and 3.4-fold changes, respectively) with the lower $V_{\max} - K_m$ kinase (experiment 3). The inclusion of 60 mM Cl^- (buffer A) caused a similar decrease in the K_i of PDK2 for ADP and the K_m for ATP (experiment 3, Table 1). Figure 2 shows that AMP-PNP is a potent inhibitor of PDK2. The data are fit by lines indicating that AMP-PNP is a linear competitive inhibitor with a K_i of $3.1 \pm 0.7 \mu\text{M}$. As indicated below, this is similar to the affinity of PDK2 for ATP. AMP-PNP reduced ATP binding at the active site in the ATP-binding assay used below (data not shown).

The large variation in kinetic parameters in buffer A is primarily due to the E2 preparation selected and to some extent its time of storage rather than being due to the PDK2 preparation selected. The high V_{\max} and high K_m for ATP were obtained using an E2 preparation with more lipoyl groups initially reduced.⁴ The addition of proteins (preincubated together for at least 1 h) to assay mixtures containing 2 mM dithiothreitol for a 2 min treatment at 30 °C was expected to cause the difference in the proportion of reduced lipoyl groups to be small. Studies in the companion paper (39) have confirmed that to be correct (~30% of the lipoyl groups are reduced), but those studies also demonstrate that the reduction of even a small portion of the lipoyl groups of E2 during storage is important.

K_m of PDK2 for E1. Under conditions of E2-aided catalysis, the K_m for E1 cannot be measured since the E1 substrate is not free. Indeed, as will be described elsewhere,³ the initial rates measured for PDK2 activity hold constant within experimental error upon halving the E1 or diluting E2·E1 complexes to 5-fold lower concentrations. Therefore, E2 helps to provide access of a PDK to E1, and the concentration dependence for E1 in the presence of E2 does not involve standard kinetics. Here, we have evaluated the K_m for E1 of PDK2 in the absence of E2. For these studies, E1 was added in a constant volume of potassium phosphate leading to 30 mM K^+ and 16 mM phosphate in all assays. Figure 3 shows results from an experiment in which both ATP and E1 were varied. The data establish that the PDK2 reaction is a sequential reaction (not a ping-pong reaction). In a double reciprocal plot the crossover point for the lines within experimental error intercepted on the x axis at $\sim 255 \mu\text{M}^{-1}$; this result implies the $K_m = K_d$ for ATP = $\sim 4 \mu\text{M}$. Because that intercept is so far to the left of the x axis in a double reciprocal plot, the data are presented in a more compact Hanes–Woolf plot. On the basis of the common intersection of lines on the x axis at $[\text{ATP}] = \sim 3.9 \mu\text{M}$, the same estimates for K_m and K_d of $\sim 4 \mu\text{M}$ for ATP are obtained when catalysis is not aided by E2. Even in the

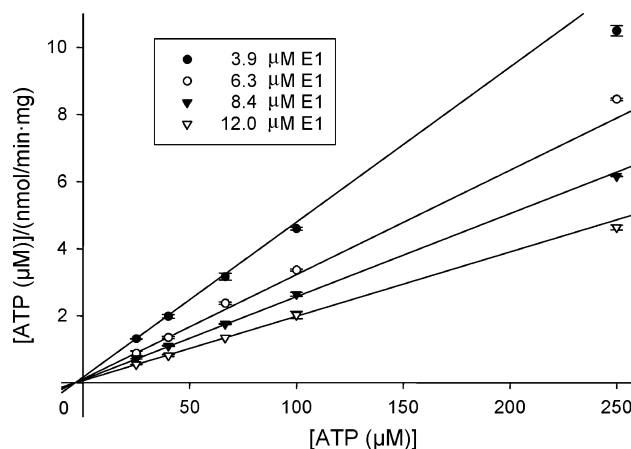


FIGURE 3: Hanes–Woolf plot of changes in PDK2 rates with variation in ATP at different fixed levels of E1. PDK2 assays were conducted in buffer A in the absence of E2, with 0.4 μg of PDK2 with E1 using 3.91, 6.26, 8.38, and 11.95 μM with the indicated levels of $[\gamma\text{-}^{32}\text{P}]\text{ATP}$. Other conditions were as described under Experimental Procedures.

presence of E2, a similar affinity (K_d) of PDK2 for ATP is estimated in ATP binding studies below. A replot of the intercepts⁵ from the reciprocal plot gives a K_m of PDK2 of $\sim 26 \mu\text{M}$ for E1 and a V_{\max} of $\sim 170 \text{ nmol}\cdot\text{min}^{-1}\cdot\text{mg}^{-1}$ ($k_{\text{cat}} = \sim 0.26 \text{ s}^{-1}$). The probable experimental error for all of these values is about $\pm 25\%$. The large error range is due to the data being collected using E1 concentrations that are below the K_m for E1. The K_m for E1 implies that $>90\%$ saturation with E1 would not be achieved until E1 is present at $>200 \mu\text{M}$ (30.6 mg/mL E1). However, $>94\%$ saturation is achieved in the presence of E2 at $0.5 \mu\text{M}$ E1.³ Therefore, the requirement for E1 is reduced by >400 -fold when E1 and PDK2 are bound by E2.

Effects of Pyruvate and Pyruvate plus ADP on PDK2 Activity. Studies evaluating pyruvate inhibition of PDK2 activity were conducted using E1 that had been rigorously prepared free of TPP as previously described (16). Substrate cannot bind to an α -keto acid dehydrogenase complex E1, unless aided by bound TPP (32–35). This prevents pyruvate from being used as a substrate by E1 to acetylate lipoyl groups of E2. In buffer B, pyruvate inhibition was very weak (data not shown). In buffer A, with 0.5, 1.0, 3.0, 5.0, and 10.0 mM pyruvate, respectively, and 0.1 mM ATP, the kinase activity remaining was 35.5%, 22.3%, 10.0%, 8.8%, and 5.55%. These values curve off in a Dixon plot in a manner characteristic of a partial inhibitor (data not shown). However, a Dixon plot for inhibition by ≤ 0.3 mM pyruvate (Figure 4A) does not show the expected (partial inhibitor) pattern of less than linear increase in inhibition with increasing pyruvate. The same data are presented in recipro-

⁴ The gel filtration step in the preparation of E2 included 10 mM mercaptoethanol rather than 1 mM mercaptoethanol. In each case that step is followed by pelleting (centrifugation at 35000 rpm in a 50.2 Ti angle rotor for 4 h) and resuspending E2 in a buffer (50 mM phosphate, pH 7.2, 0.5 mM EDTA) lacking any thiol. This approach leaves a small portion ($<15\%$) as compared to a very small ($<5\%$) portion of the lipoyl groups in the reduced form. These are estimated by acetylation of dihydrolipoyl groups using $[1\text{-}^{14}\text{C}]\text{acetyl-CoA}$ and CoA removal by the α -ketoglutarate dehydrogenase complex (25). All of the assays involved adding protein components that had been incubated for at least 1 h as a concentrate in the presence of 0.3–0.4 mM dithiothreitol (oxidation state unknown), which was introduced with E1 that was prepared in a buffer containing 1 mM dithiothreitol. For each assay the proteins were added to assay mixtures containing 2.0 mM dithiothreitol for 2 min at 30 °C.

⁵ For an order bisubstrate reaction in which ATP binds before E1 [supported by the data in this and the companion paper (39)], the standard rate equation is $v = V_{\max}/((K_{\text{dA}}K_{\text{mB}}/[\text{A}][\text{B}]) + (K_{\text{mA}}/[\text{A}]) + (K_{\text{mB}}/[\text{B}] + 1))$ which in the reciprocal form $1/v = 1/V_{\max} + (1/V_{\max}) \cdot ((K_{\text{dA}}K_{\text{mB}}/[\text{A}][\text{B}]) + (K_{\text{mA}}/[\text{A}]) + (K_{\text{mB}}/[\text{B}] + 1))$. When $[\text{A}]$ is varied at different fixed levels of $[\text{B}]$, the common intercept (independent of $[\text{B}]$) occurs where $1/[\text{A}] = -1/K_{\text{dA}}$, and for either substrate varied at different fixed levels of the other, $1/v = (1 - (K_{\text{dA}}/K_{\text{mA}}))/V_{\max}$ at the common intercept. For the Hanes–Woolf equation this rearranges to $[\text{A}]/v = ([\text{A}]/V_{\max})(1 + K_{\text{mB}}/[\text{B}]) + (K_{\text{mA}}/V_{\max})(1 + K_{\text{dA}}K_{\text{mB}}/K_{\text{mA}}[\text{B}])$, and at the common intercept, $[\text{A}] = K_{\text{dA}}$ and if this is on the x axis also equals K_{mA} . Other kinetic constants must be obtained from replots of slopes and intercepts versus $1/[\text{B}]$.

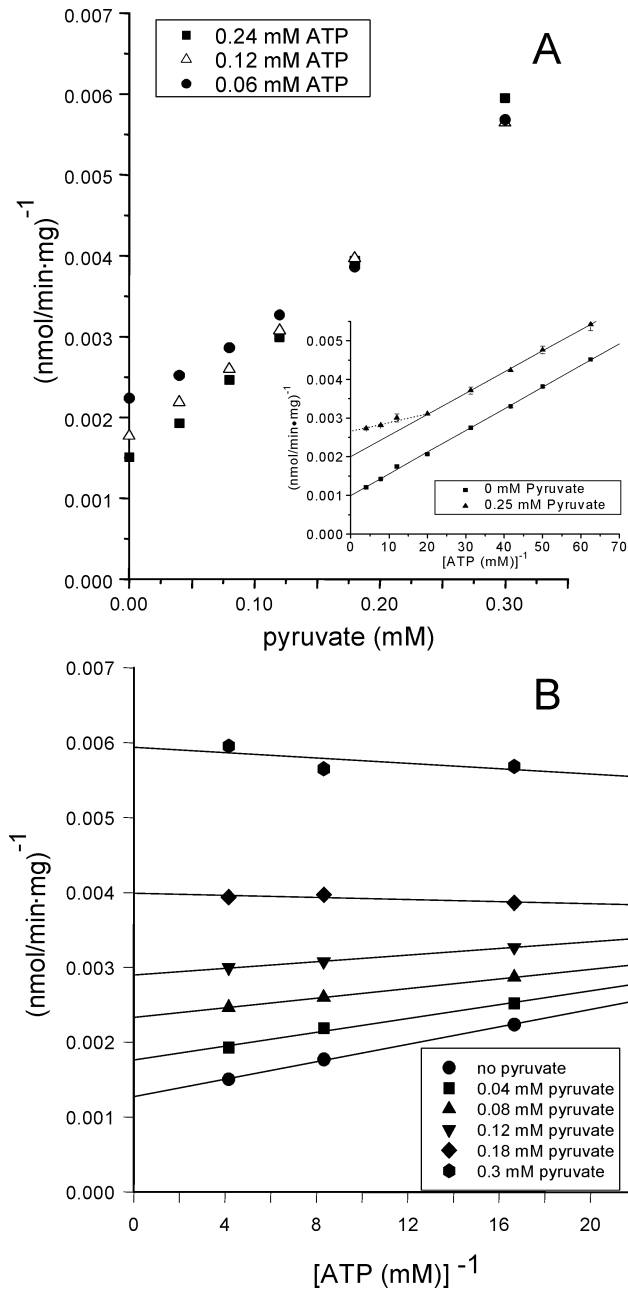


FIGURE 4: Change in PDK2 activity with variation in the level of pyruvate at different ATP levels analyzed in a Dixon plot (panel A) and double reciprocal plot (panel B). PDK2 activity was measured in buffer A using E1 completely free of TPP, with the same level of components as used in Figure 2 and the indicated concentrations of pyruvate and $[\gamma\text{-}^{32}\text{P}]\text{ATP}$. The inset shows a double reciprocal plot for a study with a wide range of ATP concentrations with no and 250 μM pyruvate.

cal plots in Figure 4B; an uncompetitive inhibition pattern is exhibited at low levels of pyruvate, but there is little or no increase in kinase activity with increasing ATP concentration at high pyruvate. This indicates that the higher pyruvate levels induce substrate inhibition by ATP. When a greater number ATP concentrations were used, the pattern at a high pyruvate level fit uncompetitive inhibition at the lower levels of ATP; however, at higher ATP levels, 0.25 mM pyruvate appeared to induce substrate inhibition by ATP (inset, Figure 4A). From a replot of the intercepts from the lower levels of pyruvate in Figure 4B, a K_i for pyruvate is estimated to be $\sim 95 \mu\text{M}$.

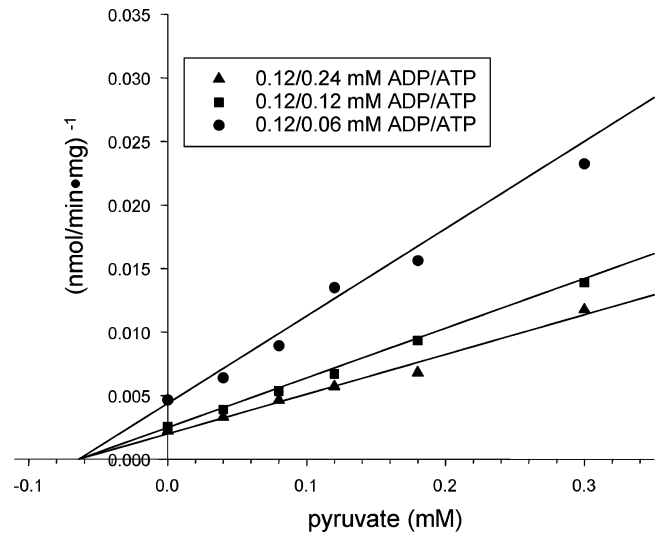


FIGURE 5: Dixon plot of pyruvate inhibition in the presence of 0.120 mM ADP at three levels of ATP. Assays were conducted with the level of components as indicated in Figure 4 at the indicated levels of pyruvate and 0.120 mM ADP with 0.60, 0.120, or 0.240 mM $[\gamma\text{-}^{32}\text{P}]\text{ATP}$.

The uncompetitive inhibition pattern indicates that pyruvate does not bind to free PDK2. A similar inhibition pattern, but with weaker inhibition, was observed with dichloroacetate (data not shown). The patterns for pyruvate and dichloroacetate inhibition are consistent with inhibitor binding to $\text{PDK2}\cdot\text{ATP}$ and $\text{PDK2}\cdot\text{ADP}$. As predicted by that possibility and observed previously with bovine PDKs (20), addition of a fixed level of ADP changed the pattern of inhibition to noncompetitive. The Dixon plot in Figure 5 shows a pattern of noncompetitive inhibition by pyruvate when PDK2 activity was measured at three levels of ATP and a fixed level of ADP. This reveals that a $\text{PDK2}\cdot\text{ADP}\cdot\text{pyruvate}$ dead-end complex was formed. Since the lines in the Dixon plot (Figure 5) extrapolate in a linear manner to the points in the absence of added pyruvate, this indicates that there is no change in the relative ratio of the K_i for ADP to K_m for ATP due to pyruvate. Thus, these results support pyruvate also binding to $\text{PDK2}\cdot\text{ATP}$. In combination with the finding that ADP is a competitive inhibitor of ATP, the results indicate an ordered reaction mechanism in which ATP binds first and ADP dissociates last (see overall analysis below).

PDK2 activity was synergistically inhibited by subsaturating ADP and pyruvate. For instance, with 240 μM ATP, 120 μM ADP only caused 32% inhibition and 40 and 80 μM pyruvate gave 22% and 39% inhibition. Assuming additive inhibition, the combination of ADP and these levels of pyruvate are predicted to give 47% and 58.5% inhibition; however, 67.5% and 74% inhibition were observed. This again fits the accumulation of a $\text{PDK2}\cdot\text{ADP}\cdot\text{pyruvate}$ dead-end complex. Similar results were previously observed with bovine kidney PDKs (20); however, PDK2 differs in that pyruvate inhibition is more potent than with dichloroacetate inhibition (16) and in undergoing ATP-induced substrate inhibition at high pyruvate.

Binding of ATP and Retention of ATP and ADP during the PDK2 Reaction. Cold trapping allows bound adenine nucleotide to be captured on PDK2 and to wash away free nucleotide. Using 0.1 mM $[\alpha\text{-}^{32}\text{P}]\text{ATP}$, binding of ATP was directly proportional to the level of PDK2 (inset to Figure

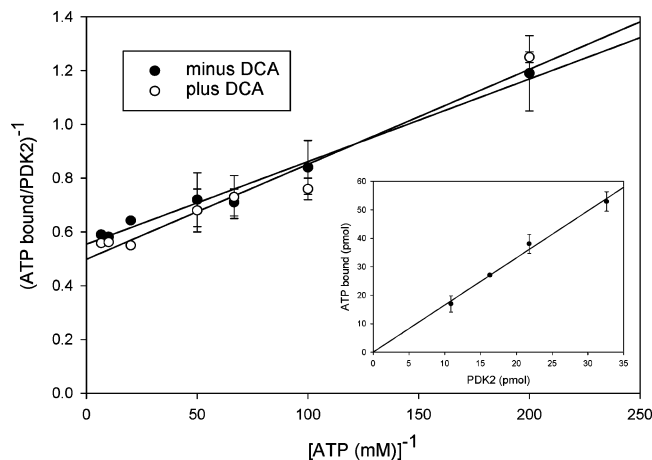


FIGURE 6: Klotz plot of binding of $[\alpha\text{-}^{32}\text{P}]\text{ATP}$ by PDK2 in the presence and absence of 0.5 mM dichloroacetate. Binding of ATP was evaluated with 2 μg of PDK2 and 18 μg of E2 using the conditions and workup described under Experimental Procedures. The inset shows binding by 1.0, 1.5, 2.0, and 3.0 μg of PDK2 using 18 μg of E2 and 0.1 mM $[\alpha\text{-}^{32}\text{P}]\text{ATP}$.

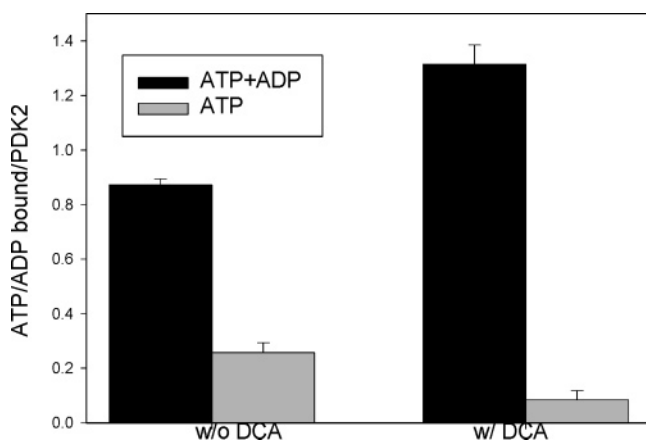


FIGURE 7: Effect of catalytic turnover on the level of bound adenine nucleotides in the presence and absence of dichloroacetate. The level of $[\gamma\text{-}^{32}\text{P}]\text{ATP}$ and $\alpha\text{-}^{32}\text{P}$ -labeled ATP and ADP retained by PDK2 was determined with 2 μg of PDK2, 39 μg of E2, and 39 μg of E1 after 25 s of PDK2 catalysis at 22 $^{\circ}\text{C}$. Binding was determined as described under Experimental Procedures.

6). Figure 6 shows a Klotz plot for binding studies in which the concentration of ATP was varied in the presence or absence of dichloroacetate. A K_d of $5.5 \pm 3 \mu\text{M}$ and an $n = \sim 1.85$ was estimated in the absence of dichloroacetate. With 0.5 mM dichloroacetate included, the results were within experimental error unchanged, but slightly higher values were estimated ($K_d = 7.7 \pm 3 \mu\text{M}$ and $n = \sim 2$). We have performed several such binding studies and typically have observed somewhat lower values for K_d and n [e.g., control curve in Figure 7 of the companion paper (39), $K_d = 4 \pm 1 \mu\text{M}$ and $n = 1.6$]. The estimates of K_d agree closely with the K_d of PDK2 for ATP derived from the kinetic studies in the absence of E2 (above). The extent of binding indicates that both binding sites on a PDK2 dimer can simultaneously bind ATP.

In the absence of E1, there was equivalent binding by PDK2 of $[\alpha\text{-}^{32}\text{P}]\text{ATP}$ and $[\gamma\text{-}^{32}\text{P}]\text{ATP}$, and treatment of the washed membrane with 2.5 mL of 5% formic acid fully released the kinase-bound ATP. To maintain initial velocity conditions at 22 $^{\circ}\text{C}$ with 2 μg of PDK2, E1 and E2 were each increased to 39 μg and a reaction time of ≤ 25 s. Under

conditions of maximum catalysis (no ADP added), about 72% of the bound adenine nucleotide was ADP, based on the difference between the levels bound when $[\alpha\text{-}^{32}\text{P}]\text{ATP}$ and $[\gamma\text{-}^{32}\text{P}]\text{ATP}$ were used (Figure 7). Inclusion of DCA during turnover increased the portion of adenine nucleotides bound as ADP to $\sim 94\%$ (Figure 7). Therefore, there is a transition from ~ 2.6 to ~ 16 times as much ADP as ATP bound. This agrees with the kinetic studies (see overall analysis below) and establishes that under conditions of turnover the PDK2 \cdot ADP \cdot DCA complex accumulates. At -3°C , PDK2 does not catalyze one round of turnover in the time required to complete the washing away of free ATP.

CoA Inhibition. Modest CoA inhibition of bovine PDK has been observed in the phosphorylation of E1 in the absence of E2 (36). Near-maximal CoA inhibition ($31 \pm 2\%$) of E2-activated PDK2 activity was achieved with 5 μM CoA. Half-maximal inhibition was observed with about 2 μM CoA. CoA inhibition was not due to disulfide formation. The CoA concentrates were prepared in the presence of 0.5 mM DTT and 5 mM cysteine and were diluted 10-fold in the final assay mixtures; this condition was repeated in the control assay. CoA inhibition was also observed in the absence of E2. The observed inhibition suggests that there is an independent binding site for CoA on PDK2. It seems surprising that such a high-affinity site would exist for supporting such a modest inhibition. Studies testing for a synergistic inhibition by CoA and either pyruvate and ADP or the combination failed to detect such an effect.

Analysis of Kinetic Results. Inclusion of K^+ , Cl^- , and phosphate at nearly physiological levels led to decreased affinities of ATP and ADP for PDK2. At the same time, elevation of these ions is critical for observing strong inhibition by pyruvate of PDK2 as well as effective stimulation of this kinase by NADH and acetyl-CoA [companion paper (39)]. These observations suggested that regulation may operate through altering a common rate-limiting step.

In the presence of E2, we cannot vary E1 and derive normal kinetic information. In the absence of E2, a sequential mechanism is supported; however, kinetic parameters that might be expected to be similar are very different. In the absence of E2, the K_m for ATP is much lower and close to the values estimated for the K_d for ATP binding as determined both in that kinetic study and in "cold-trap" binding studies with E2-bound PDK2. With E2-activated PDK2, an increase k_{cat} was invariably accompanied by an increase in the K_m of PDK2 for ATP, and the ratio tends to remain relatively constant. This trend is further supported in the companion paper under conditions of product stimulation. These observations are most easily explained and fit by PDK2 catalyzing an ordered reaction mechanism in which ATP binds first because $K_m = k_{\text{cat}}/k_1$ for the first substrate. The constancy of the k_{cat}/K_m ratio as the K_m for ATP and k_{cat} values increase additionally indicates that kinetic rate constants other than k_1 contribute to the change in these kinetic parameters. Only an ordered reaction with ATP binding first can easily fit the combination of a constant k_{cat}/K_m , ADP being a competitive inhibitor of ATP and addition of ADP transforming pyruvate inhibition from being an uncompetitive inhibitor versus ATP to a noncompetitive versus ATP.

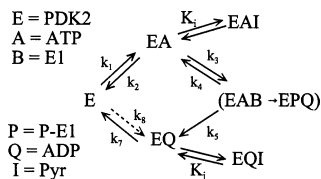


FIGURE 8: Reaction scheme for an ordered reaction with binding of the inhibitor (I) to the EA and EQ reaction intermediates. The kinetic rate constants for the forward and reverse steps are indicated. Inhibition constants for equilibrium binding of the inhibitor to form the dead-end complexes, EAI and EQI, are also indicated; however, our kinetic studies yield inhibition constants (K_i in the text) that reflect inhibitor binding to both EA and EQ.

For E2-activated PDK2, alternative sequential mechanisms can be eliminated. An ordered mechanism in which E1 would bind first does not fit ADP being a competitive inhibitor versus ATP. Analytical ultracentrifugation studies detected a very small equilibrium binding effect for stronger binding of PDK2 to E2·E1 than to E2 (28). If a rapid-equilibrium random mechanism was operating, a large difference in PDK2 binding to E2 and E2·E1 would be expected since there rapid encounters between PDK2 and E1 should occur with both components being bound on neighboring mobile domains at the E2 surface. Indeed, E1 is saturating for E1-aided PDK2 catalysis at the levels used in the present study.³

Several observations support ADP dissociation being rate limiting in E2-activated PDK2 catalysis. Binding studies detected a major portion of bound ADP under conditions of turnover in the absence of added ADP. Uncompetitive pyruvate inhibition in the absence of added ADP fits binding to PDK2·ADP (and PDK2·ATP). The capacity for synergistic inhibition by ADP plus pyruvate and the transition upon adding ADP to pyruvate acting as a noncompetitive inhibitor definitively support formation of appreciable levels of the PDK2·ADP·pyruvate complex. Under conditions of turnover, the substantial increase in the level of bound ADP due to the addition of dichloroacetate fits the dissociation of ADP being further forestalled by formation of the PDK2·ADP·dichloroacetate dead-end complex. The finding that product stimulation reduces bound nucleotides [companion paper (39)] is also consistent with an increase in a rate-limiting dissociation of ADP.

For the following analysis, we will use the Cleland format for defining rate constants (37) in which the rate constants for the forward reaction steps have odd-numbered subscripts and those for the reverse reaction steps have even-numbered subscripts (rather than negative). Figure 8 presents a simple reaction scheme for an ordered reaction with pyruvate binding to PDK2·ATP or PDK2·ADP. Besides the relatively constant k_1 , only k_5 and k_7 appear in $k_{\text{cat}} = k_5 k_7 / (k_5 + k_7)$ or $K_m = k_5 k_7 / k_1 (k_5 + k_7)$. An increase in the rate of ADP dissociation (k_7 step) would lead to an increase in both V_{max} and K_m based on the above equations if the reaction and dissociation of phosphorylated E1 (k_5 step) is several-fold faster than ADP dissociation. This is in accord with the nearly equivalent changes in these parameters.

With the transition from buffer B to buffer A, along with the decrease in V_{max} , K_i for ADP, and K_m for ATP (Table 1), there is a gain in capacity to stimulate PDK2 activity (39). In an ordered mechanism, these can arise from slower dissociation of ADP, but k_5 must be at least 4-fold faster than k_7 to explain the higher level of bound ADP than ATP

during turnover (Figure 7) as well as the capacity to stimulate PDK2 activity (39). With the ordered mechanism and using the typical values from experiments 3 and 4 in Table 1, $k_{\text{cat}}/K_m = k_1 = 2.3 \times 10^4 \text{ M}^{-1} \text{ s}^{-1}$, the rate constant for a rate-limiting dissociation of ADP, k_7 , must be $\geq k_{\text{cat}} = 0.91 \pm 0.08 \text{ s}^{-1}$ ($k_{\text{cat}} = k_7$ when $k_5 \gg k_7$) and k_7 cannot exceed 1.14 s^{-1} if $k_5 \geq 4 \times k_7$. With the above value for k_1 and $K_d \approx 5 \mu\text{M}$, we can estimate that $k_2 = \sim 0.12 \text{ s}^{-1}$ so that dissociation of ATP is predicted to be much slower than $k_{\text{cat}} = 0.91 \text{ s}^{-1}$. However, the rate of the dissociation step does not affect the forward reaction rate in an ordered reaction. The low value of k_2 predicts that some mechanism hinders ATP dissociation. This is consistent with the capacity to measure ATP binding by cold trapping. Structural studies on PDK2 indicate that Phe318/Gly319 move into a position that hinders dissociation of adenine nucleotides (11, 38); this may be the stabilized carbonyl group of Gly319 interacting with a bound K^+ , as found with the branched chain kinase (12).

Induced substrate inhibition by high levels of pyruvate (Figure 4) may result from the PDK2·ATP·pyr using E1 as a substrate followed by dissociation of phosphorylated E1 producing PDK2·ADP·pyr from which free kinase is generated slowly. The latter complex would regenerate free PDK2 slowly. Particularly at high ATP and high pyruvate, this alternative reaction pathway may be favored. Given the large number of kinetic variables that this alternative reaction pathway introduces, a simulation of such a mechanism could be performed, but almost certainly multiple solutions will fit the data so little insight would be gained.

Structural studies (11, 38) reveal that major conformational changes occur in PDK2 upon binding of ATP or ADP. It seems likely that these prominent adjustments around the active site convert PDK2 to a conformation with an increased capacity to productively interact with the E1 substrate. AMP-PNP was shown to be a strong competitive inhibitor of ATP with a K_i that is very close to the K_d determined for ATP in the cold-trap binding studies and kinetic studies in the absence of E2. It seems likely that AMP-PNP induces a similar conformational change in PDK2 as ATP. In AUC studies, the addition of AMP-PNP reduced somewhat PDK2 binding to E2·E1 (28). A productive interaction after binding of ATP or AMP-PNP need not involve a tight affinity of PDK2 for E1. In the crystal structure of E1, the first site of phosphorylation (essentially the only site undergoing phosphorylation in our initial velocity studies here) is not exposed at the surface of E1 (34). Similarly the γ -phosphate of ATP would not appear to be well exposed in the PDK2 structure (38). These structures suggest that, prior to phosphorylation of site 1, binding energy will be needed to force conformational changes that produce an open interface between the γ -phosphate of ATP and site 1 on E1. Such an expense in binding energy would not contribute to equilibrium binding of PDK2 to E1. Further studies will be needed to evaluate this suggestion that the interaction of ATP alters PDK2 structure in a way that favors rapid catalysis but with a cost in binding affinity as indicated by comparing binding of PDK2 and PDK2 (AMP-PNP) to E2·E1 (28).

In the absence of E2 even if PDK2·ATP is tightly held and poised to react, PDK2 has a high K_m of $26 \mu\text{M}$ for E1, and E1 availability limits PDK2 activity at the levels of E1 ($< 2 \text{ mg/mL}$) that we have used. However, we have found that E2 reduces the requirement for E1 by at least 400-fold

and removes this limitation leading to ADP dissociation being a slow step. Our results and studies on effects of adenine nucleotides on binding of PDK2 to E2 (28) indicate that there are reversible avenues of communication between the active site and effector sites. ADP binding must change the pyruvate/dichloroacetate site to enhance inhibitor binding. Binding of these effectors apparently then alters or stabilizes a conformational state at the active site that hinders ADP dissociation.

Overall, our results support E2-activated catalysis in the presence of physiological salts being limited by ADP dissociation which favors the development of pyruvate inhibition by binding to this intermediate. When a low-energy state elevates intramitochondrial ADP, this mechanism favors potent inhibition of PDK2 by pyruvate acting in combination with ADP. This regulation then supports the desired outcome of elevating the level of active PDC under conditions of low energy and good substrate availability.

ACKNOWLEDGMENT

We thank Dr. Yasuaki Hiromasa and John Kurche for making some of the E2 preparations used in this study.

REFERENCES

- Patel, M. S., and Roche, T. E. (1990) Molecular biology and biochemistry of pyruvate dehydrogenase complexes, *FASEB J.* **4**, 3224–3233.
- Roche, T. E., Baker, J., Yan, X., Hiromasa, Y., Gong, X., Peng, T., Dong, J., Turkan, A., and Kasten, S. A. (2001) Distinct regulatory properties of pyruvate dehydrogenase kinase and phosphatase isoforms, *Prog. Nucleic Acid Res. Mol. Biol.* **70**, 33–75.
- Randle, P. J. (1986) Fuel selection in animals, *Biochem. Soc. Trans.* **14**, 799–806.
- Randle, P. J., and Priestman, D. A. (1996) Shorter term and longer term regulation of pyruvate dehydrogenase kinases, in *Alpha-Keto Acid Dehydrogenase Complexes* (Patel, M. S., Roche, T. E., and Harris, R. A., Eds.) pp 151–161, Birkhauser Verlag, Basel.
- Sugden, M. C., and Holness, M. J. (1996) Hormonal and nutritional modulation of PDHC activity status, in *Alpha-Keto Acid Dehydrogenase Complexes* (Patel, M. S., Roche, T. E., and Harris, R. A., Eds.) pp 163–176, Birkhauser Verlag, Basel.
- Harris, R. A., Huang, B., and Wu, P. (2001) Control of pyruvate dehydrogenase kinase gene expression, *Adv. Enzymol. Regul.* **41**, 269–288.
- Gudi, R., Bowker-Kinley, M. M., Kedishvili, N. Y., Zhao, Y., and Popov, K. M. (1995) Diversity of the pyruvate dehydrogenase kinase gene family in humans, *J. Biol. Chem.* **270**, 28989–28994.
- Rowles, J., Scherer, S. W., Xi, T., Majer, M., Nickle, D. C., Rommens, J. M., Popov, K. M., Harris, R. A., Riebow, N. L., Xia, J., Tsui, L.-C., Bogardus, C., and Prochazka, M. (1996) Cloning and characterization of PDK4 on 7q21.3 encoding a fourth pyruvate dehydrogenase kinase isozyme in human, *J. Biol. Chem.* **271**, 22376–22382.
- Bowker-Kinley, M., and Popov, K. M. (1999) Evidence that pyruvate dehydrogenase kinase belongs to the ATPase/kinase superfamily, *Biochem. J.* **344**, 47–53.
- Wynn, R. M., Chuang, J. L., Cote, C. D., and Chuang, D. T. (2000) Tetrameric assembly and conservation in the ATP-binding domain of rat branched-chain alpha-ketoacid dehydrogenase kinase, *J. Biol. Chem.* **275**, 30512–30519.
- Steussy, C. N., Popov, K. M., Bowker-Kinley, M. M., Sloan, R. B., Harris, R. A., and Hamilton, J. A. (2001) Structure of pyruvate dehydrogenase kinase. Novel folding pattern for a serine protein kinase, *J. Biol. Chem.* **276**, 37443–37450.
- Machius, M., Chuang, J. L., Wynn, R. M., Tomchick, D. R., and Chuang, D. T. (2001) Structure of rat BCKD kinase: Nucleotide-induced domain communication in a mitochondrial protein kinase, *Proc. Natl. Acad. Sci. U.S.A.* **98**, 11218–11223.
- Lawson, J. E., Niu, X.-D., Browning, K. S., Trong, H. L., Yan, J., and Reed, L. J. (1993) Molecular cloning and expression of the catalytic subunit of bovine pyruvate dehydrogenase phosphatase and sequence similarity with protein phosphatase 2C, *Biochemistry* **32**, 8987–8993.
- Huang, B., Gudi, R., Wu, P., Harris, R. A., Hamilton, J., and Popov, K. M. (1998) Isozymes of pyruvate dehydrogenase phosphatase. DNA-derived amino acid sequences, expression, and regulation, *J. Biol. Chem.* **273**, 17680–17688.
- Bowker-Kinley, M. M., Davis, W. I., Wu, P., Harris, R. A., and Popov, K. M. (1998) Evidence for existence of tissue-specific regulation of the mammalian pyruvate dehydrogenase complex, *Biochem. J.* **329**, 191–196.
- Baker, J. C., Yan, X., Peng, T., Kasten, S. A., and Roche, T. E. (2000) Marked differences between two isoforms of human pyruvate dehydrogenase kinase, *J. Biol. Chem.* **275**, 15773–15781.
- Korotchkina, L. G., and Patel, M. S. (2001) Site specificity of four pyruvate dehydrogenase kinase isozymes toward the three phosphorylation sites of human pyruvate dehydrogenase, *J. Biol. Chem.* **279**, 37223–37229.
- Roche, T. E., Hiromasa, Y., Turkan, A., Gong, X., Peng, T., Yan, X., Kasten, S. A., Bao, H., and Dong, J. (2003) Lipoyl domain-facilitated activation and control of pyruvate dehydrogenase kinases and phosphatase isoform 1, *Eur. J. Biochem.* **270**, 1050–1056.
- Wu, P., Blair, P. V., Sato, J., Jaskiewicz, J., Popov, K. M., and Harris, R. A. (2000) Starvation increases the amount of pyruvate dehydrogenase kinase in several mammalian tissues, *Arch. Biochem. Biophys.* **381**, 1–7.
- Pratt, M. L., and Roche, T. E. (1979) Mechanism of pyruvate inhibition of kidney pyruvate dehydrogenase, kinase and synergistic inhibition by pyruvate and ADP, *J. Biol. Chem.* **254**, 7191–7196.
- Hucho, F., Randall, D. D., Roche, T. E., Burgett, M. W., Pelley, J. W., and Reed, L. J. (1972) α -keto acid dehydrogenase complexes. XVII. kinetic and regulatory properties of pyruvate dehydrogenase kinase and pyruvate dehydrogenase phosphatase from bovine kidney and heart, *Arch. Biochem. Biophys.* **151**, 328–340.
- Whitehouse, S., Cooper, R. H., and Randle, P. J. (1974) Mechanism of activation of pyruvate dehydrogenase by dichloroacetate and other halogenated carboxylic acids, *Biochem. J.* **141**, 761–774.
- Hiromasa, Y., Fujisawa, T., Aso, Y., and Roche, T. E. (2004) Organization of the cores of the mammalian pyruvate dehydrogenase complex formed by E2 and E2 plus the E3-binding protein and their capacities to bind the E1 and E3 components, *J. Biol. Chem.* **279**, 6921–6933.
- Cate, R. L., and Roche, T. E. (1978) A unifying mechanism for stimulation of mammalian pyruvate dehydrogenase kinase activity by NADH, dihydrolipoamide, acetyl coenzyme A, or pyruvate, *J. Biol. Chem.* **253**, 496–503.
- Rahmatullah, M., and Roche, T. E. (1985) Modification of bovine kidney pyruvate dehydrogenase kinase activity by CoA esters and their mechanism of action, *J. Biol. Chem.* **260**, 10146–10152.
- Ravindran, S., Radke, G. A., Guest, J. R., and Roche, T. E. (1996) Lipoyl domain-based mechanism for integrated feedback control of pyruvate dehydrogenase complex by enhancement of pyruvate dehydrogenase kinase activity, *J. Biol. Chem.* **271**, 653–662.
- Popov, K. M. (1997) Regulation of mammalian pyruvate dehydrogenase kinase, *FEBS Lett.* **419**, 197–200.
- Hiromasa, Y., and Roche, T. E. (2003) Facilitated interaction between the pyruvate dehydrogenase kinase isoform 2 and the dihydrolipoyl acetyltransferase, *J. Biol. Chem.* **278**, 33681–33693.
- Roche, T. E., and Reed, L. J. (1974) Monovalent cation requirement for ADP inhibition of pyruvate dehydrogenase kinase, *Biochem. Biophys. Res. Commun.* **59**, 1341–1348.
- Robertson, J. G., Barron, L. I., and Olson, M. S. (1989) Bovine heart pyruvate dehydrogenase kinase stimulated by monovalent ions, *J. Biol. Chem.* **264**, 11626–11631.
- Liu, T.-C., Korotchkina, L. G., Hyatt, S. L., Vettakkorumakankav, N. N., and Patel, M. S. (1995) Spectroscopic studies of the characterization of recombinant human dihydrolipoamide dehydrogenase and its site-directed mutants, *J. Biol. Chem.* **270**, 15545–15550.
- Evarsson, A., Seger, K., Turley, S., Sokatch, J. R., and Hol, W. G. (1999) Crystal structure of 2-oxoisovalerate and dehydrogenase and the architecture of 2-oxo acid dehydrogenase multienzyme complexes, *Nat. Struct. Biol.* **6**, 785–792.
- Wynn, R. M., Ho, R., Chuang, J. L., and Chuang, D. T. (2001) Roles of the active site and novel K⁺ ion-binding site residues in

- human mitochondrial branched chain α -keto acid decarboxylase/dehydrogenase, *J. Biol. Chem.* 276, 4168–4174.
34. Ciazak, E. M., Korotchkina, L. G., Dominiak, P. M., Sidhu, S., and Patel, M. S. (2003) Structural basis for flip-flop action of thiamin pyrophosphate-dependent enzymes revealed by human pyruvate dehydrogenase, *J. Biol. Chem.* 278, 21240–21246.
 35. Nakai, T., Nakagawa, N., Maoka, N., Masui, R., Kuramitsu, S., and Kamiya, N. (2004) Ligand-induced conformational changes and a reaction intermediate in branched-chain 2-oxo acid dehydrogenase (E1) from *Thermus thermophilus* HB8 as revealed by X-ray crystallography, *J. Mol. Biol.* 337, 1011–1033.
 36. Rahmatullah, M., and Roche, T. E. (1987) The catalytic requirements for reduction and acetylation of protein X and the related regulation of various forms of resolved pyruvate dehydrogenase kinase, *J. Biol. Chem.* 262, 10265–10271.
 37. Cleland, W. W. (1963) The kinetics of enzyme-catalyzed reactions with two or more substrates or products I. nomenclature and rate equations, *Biochim. Biophys. Acta* 67, 104–137.
 38. Robinson, C. M., Tarylor, W. E., Tucker, A. D., and Knoechel, T. G. (2002) Crystal structure of pyruvate dehydrogenase kinase 2 (PDHK-2) and use thereof in methods for identifying and designing new ligands, pp 1–304, Great Britain, United States, Patent EP1247860.
 39. Bao, H., Kasten, S. A., Yan, X., Hiromasa, Y., and Roche, T. E. (2004) Pyruvate dehydrogenase kinase isoform 2 activity stimulated by speeding up the rate of dissociation of ADP, *Biochemistry* 43, 13442–13451.

BI049488X